

## Monte Carlo simulation of dimensional crossover in the XY model

Wolfhard Janke

*Institut für Physik, Johannes Gutenberg-Universität Mainz, Staudinger Weg 7, 55099 Mainz, Germany*

Klaus Nather

*Institut für Theoretische Physik, Freie Universität Berlin, Arnimallee 14, 14195 Berlin, Germany*

(Received 23 July 1993)

We report Monte Carlo simulations of Villain's periodic Gaussian XY model on  $L^2 \times N$  lattices of film geometry ( $L \gg N$ ) with up to  $N=16$  layers, employing the single-cluster update algorithm combined with improved estimators for measurements. The boundary conditions are periodic within each layer and free at the bottom and top layer. Based on data for the specific heat, the spin-spin correlation function, and the susceptibility in the high-temperature phase we study the crossover from three- to two-dimensional behavior as criticality is approached. For the transition temperatures, determined from Kosterlitz-Thouless fits to the correlation length and susceptibility, we observe a pronounced scaling behavior with  $N$ . The associated critical exponent, however, deviates from theoretical expectations. More qualitatively, we further discuss the distribution and shapes of vortex loops in the crossover region.

### I. INTRODUCTION

For systems with short-range interactions the concept of universality predicts that qualitative properties of continuous phase transitions should only depend on the spatial dimension of the system and on the symmetry of the order parameter.<sup>1</sup> Mathematically, the spatial dimension is given by the number of directions in which the system extends to infinity. While this obviously can never be realized in nature, there are still many systems where finite-size corrections are experimentally so small that this mathematical idealization works perfectly. By the same argument the two long directions of films can be considered as infinite. The film thickness, on the other hand, is definitely finite and does strongly influence the behavior of the system. In fact, in contrast to the three-dimensional (3D) bulk behavior, we expect for films of finite thickness a phase transition (if at all) that can be classified according to the two-dimensional (2D) universality class.<sup>2,3</sup> More precisely we expect a crossover from 3D to 2D behavior as soon as the bulk correlation length  $\xi$  of the system approaches the order of the film thickness.<sup>2,3</sup>

Taking the Ising model as a typical example, the crossover from 3D to 2D behavior of systems with one-component order parameters has been studied numerically some time ago by Binder and Hohenberg.<sup>4</sup> While this has interesting applications to many magnetic materials there are also important physical systems that are described by a two-component order parameter, e.g., liquid helium or superconductors. Here we report Monte Carlo (MC) simulations of the crossover behavior for these systems, using the XY model as the generic representative of this universality class.<sup>5</sup> In our work we have chosen Villain's<sup>6</sup> periodic Gaussian formulation of the XY model.<sup>7</sup> Some of our results can be compared with recent

work by Schmidt and Schneider<sup>8</sup> who performed similar simulations for the cosine formulation.

### II. THE MODEL

The partition function of the periodic Gaussian XY model is given by

$$Z = \prod_{\mathbf{x}} \left[ \int_{-\pi}^{\pi} \frac{d\theta(\mathbf{x})}{2\pi} \right] \times \sum_{\{n_i(\mathbf{x})\}} \exp \left[ -\frac{\beta}{2} \sum_{\mathbf{x}, i} (\nabla_i \theta - 2\pi n_i)^2 \right], \quad (1)$$

where  $\nabla_i \theta(\mathbf{x}) \equiv \theta(\mathbf{x} + \mathbf{i}) - \theta(\mathbf{x})$  are the lattice gradients in the  $i$  direction of a cubic lattice, the integer variables  $n_i(\mathbf{x})$  run from  $-\infty$  to  $\infty$ , and  $\beta \equiv J/k_B T$  is the (reduced) inverse temperature. Films of increasing thickness were simulated by stacking  $N=1, 2, 3, 4, 6, 10$ , and 16 layers of size  $L \times L$  with  $L \gg N$  on top of each other along the  $z$  direction. The ferromagnetic coupling  $J$  was taken to be isotropic. Within each layer we took periodic boundary conditions in order to reduce finite-size effects in  $L$  as much as possible, while at the top and bottom layer we imposed free boundary conditions in the  $z$  direction.

Our choice of the periodic Gaussian formulation is motivated by the fact that the partition function (1) can exactly be transformed into a gas of topological defects with long-range interactions of the Coulomb type [9,10]. This is the main difference to the cosine formulation [with  $\exp(\beta \cos(\nabla_i \theta))$  replacing the periodic Gaussian], where the defects also interact in a complicated nonlinear way with the spin-wave excitations.<sup>11</sup> Physically the defects can be interpreted as the vortex excitations invoked in the description of liquid helium.<sup>5,10</sup> In two dimensions the defects are pointlike objects, providing the physical

picture for the renormalization-group treatment of Kosterlitz and Thouless (KT).<sup>12,13</sup> In three dimensions the defects are linelike objects. For literature on recent attempts to understand the  $\lambda$  transition in liquid helium as proliferation of these vortex lines see, e.g., Ref. [14].

The phase transitions in the limiting cases  $N=L$  (3D) and  $N=1$  (2D) have been investigated by a variety of approaches. In three dimensions, analyses of high-temperature series (HTS) expansions,<sup>15</sup> resummations of field-theoretic perturbation series,<sup>16</sup> and recent MC simulations<sup>17,18</sup> are all compatible with a conventional power-law behavior  $\xi \propto (1-\beta/\beta_c)^{-\nu}$  and  $\chi \propto (1-\beta/\beta_c)^{-\gamma}$  with critical exponents  $\nu=0.670$  and  $\gamma=1.316$ . In two dimensions, however, the situation has been quite controversial. While the KT theory predicts an exponentially diverging correlation length,<sup>13</sup>

$$\xi \propto \exp[b(1-\beta/\beta_c)^{-\nu}], \quad \nu = \frac{1}{2}, \quad (2)$$

and susceptibility  $\chi \propto \xi^{2-\eta}$  with  $\eta = \frac{1}{4}$ , alternative considerations<sup>19</sup> suggested a conventional power-law behavior with nontrivial critical exponents  $\nu$  and  $\gamma$ . To clarify this point, analyses of extended HTS expansions<sup>20</sup> and MC studies<sup>21</sup> of the cosine formulation have been performed. The results of both approaches were interpreted in favor of the KT scenario. Since no data of comparable quality were available for the periodic Gaussian XY model, we first studied the 2D limit of this formulation. From high-statistics MC simulations<sup>22,23</sup> with correlation lengths up to  $\xi \approx 140$  on large lattices of sizes up to  $1200^2$ , we obtained even stronger evidence for the KT predictions in this formulation.

### III. THE SIMULATION

In our MC simulations<sup>7</sup> of the partition function (1) we applied the  $Z_n$  approximation with  $n=100$  to the angles  $\theta(\mathbf{x})$ . This enables us to store the sums over the integer variables  $n_i(\mathbf{x})$  in a lookup table, calculated numerically for each  $\beta$  once at the beginning of the run. In this way it is then straightforward to adapt the single-cluster update algorithm<sup>24</sup> to the periodic Gaussian formulation.<sup>22</sup> Besides monitoring the peaks of the specific heat  $C$ , the main results are based on analyses of the susceptibility,

$$\chi \equiv V \left\langle \left[ \frac{1}{V} \sum_{\mathbf{x}} \vec{s}(\mathbf{x}) \right]^2 \right\rangle, \quad (3)$$

where  $\vec{s}(\mathbf{x}) \equiv (\cos\theta, \sin\theta)$  and  $V = NL^2$ , and the spin-spin correlations,

$$G(\mathbf{x}, \mathbf{x}') \equiv \langle \vec{s}(\mathbf{x}) \cdot \vec{s}(\mathbf{x}') \rangle, \quad (4)$$

in the high-temperature phase, using for the measurements variance reduced "cluster observables."<sup>25</sup> To be precise, we have measured the  $k_y=0$  momentum projection of (4),

$$g(x) \equiv \langle \hat{s}(x, z) \cdot \hat{s}(0, z) \rangle, \quad (5)$$

with  $\hat{s}(x, z) \equiv \sum_{y=1}^L \vec{s}(x, y, z)$ , along the  $x$  direction in the innermost layers and extracted the correlation length  $\xi$  from fits to a hyperbolic cosine,  $\cosh[(x-L/2)/\xi]$ ,

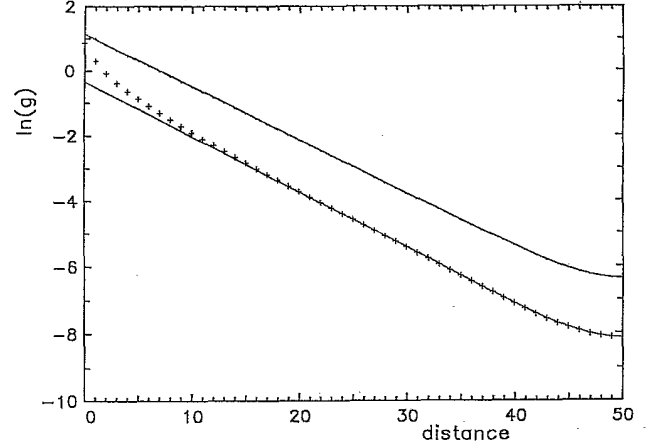


FIG. 1. Correlation functions for  $N=4$  ( $\cdot$ ) and  $N=30$  ( $+$ ) layers of size  $L \times L$  with  $L=100$ . The solid lines are fits of  $\cosh[(x-L/2)/\xi]$  through the last 20 points, yielding in both cases a correlation length of  $\xi \approx 6$ .

thereby taking into account the periodic boundary conditions in the  $x$  direction. As is demonstrated in Fig. 1, this ansatz works perfectly in the quasi-2D case of a few layers. For many layers, on the other hand, corrections are expected which modify the short-distance behavior of  $g(x)$ . The data for  $N=30$  layers in Fig. 1 show, however, that these corrections die out quite rapidly and that there is still a significant range in  $x$  over which the simple ansatz is an extremely good approximation. To reduce finite-size effects in  $L$ , we always took care that  $L \approx 6-8\xi$ . Extensive tests for the pure 2D model showed that this is a safe condition.<sup>22,23</sup>

### IV. RESULTS

To determine the transition point  $\beta_c(N)$  for each film thickness  $N$ , we first located the onset of the two-dimensional KT behavior of  $\xi$  and  $\chi$  via goodness-of-fit analyses. As a general rule we find that this is the case for  $\xi > N/2$ . Only for the thickest film with  $N=16$  lay-

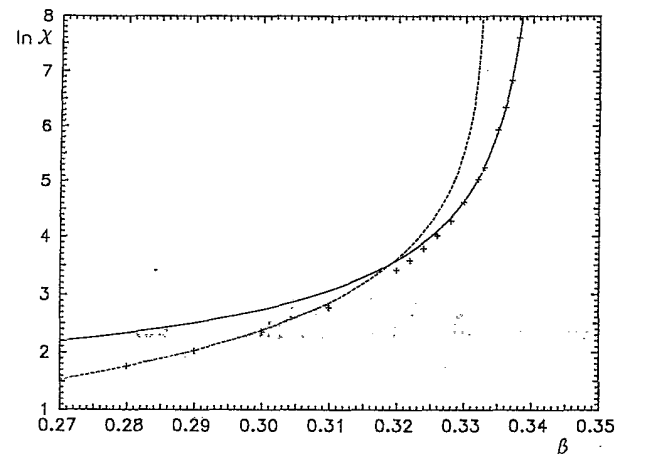


FIG. 2. Crossover from 3D power-law behavior (dashed line, using  $\gamma_{3D}=1.316$ ) to 2D KT behavior (solid line) of the susceptibility for  $N=16$  layers.

TABLE I. Inverse critical temperatures  $\beta_c(N)$  and the location of the specific-heat maximum,  $\beta_{\max}(N)$ .

$N$	$\xi(T)$	$\beta_c$ from kT fits to			$\beta_{\max}$
		$\xi(\beta)$	$\chi(T)$	$\chi(\beta)$	
1	0.754 5(54)	0.758 6(59)	0.751 0(32)	0.754 8(35)	0.538 7(19)
2	0.487 8(27)	0.490 3(30)	0.482 6(11)	0.484 4(12)	0.426 20(58)
3	0.417 14(89)	0.417 70(91)	0.419 88(60)	0.420 61(64)	0.393 79(36)
4	0.391 30(53)	0.391 72(54)	0.390 87(21)	0.391 29(22)	0.374 43(20)
6	0.365 81(92)	0.365 98(92)	0.366 23(30)	0.366 41(30)	0.358 29(11)
10	0.349 67(23)	0.349 74(24)	0.349 85(12)	0.349 92(12)	0.345 77(15)
16	0.342 25(60)	0.342 28(64)	0.341 86(25)	0.341 89(25)	0.339 76(18)

ers, we start seeing a region with 3D bulk behavior; see Fig. 2. It is tempting to identify this 3D region with  $\xi < N/10$ , but even for  $N=16$  layers this is, of course, still perturbed by nonuniversal lattice corrections. Having determined the region of 2D behavior, we then fitted the data for  $\xi$  and  $\chi$  to the KT prediction (2) and the corresponding formula for  $\chi$ , respectively. In these fits we thus always kept  $\nu = \frac{1}{2}$  fixed at its theoretical value. As a test for systematic errors (due to omitted correction terms) we also used (2) rewritten as a function of  $T$ . Depending on  $N$ , the number of data points included in the fits was 5 or 6, with a maximal correlation length between 26 and 46 for  $N \geq 2$ , requiring layers of sizes of the order of  $200^2$  to  $400^2$ . For each film thickness  $N$  these fits provided us with four estimates of  $\beta_c(N)$  compiled in Table I. The values for a single layer deviate slightly from our earlier results in Ref. 22, since in the present fits we used only the five data points with the largest correlation length.

According to Fisher's scaling prediction<sup>2,3</sup> the  $\beta_c(N)$  should scale asymptotically for large  $N$  as

$$\beta_c(N) = \beta_c^{3D} + cN^{-\lambda}, \quad (6)$$

with  $c$  being a constant and

$$1/\lambda = \nu_{3D} = 0.670 \pm 0.002. \quad (7)$$

Here  $\beta_c^{3D} \equiv \beta_c(\infty)$  is the critical coupling of the 3D bulk system and  $\nu_{3D}$  is the bulk correlation length exponent. The results of three-parameter fits to (6) for each of the four sets of  $\beta_c(N)$  values given in Table I [labeled according to the type of KT fit used to determine  $\beta_c(N)$ ] are collected in Table II. In these fits all points with  $N \geq 2$  are taken into account. In Fig. 3 we plot  $\beta_c(N) - \beta_c^{3D}$  with  $\beta_c^{3D} = 0.334$  vs  $N$  on a log-log scale. We see that the critical couplings do indeed scale quite nicely down to remarkably small values of  $N$ . The solid curve is

a straight line corresponding to the exponent

$$1/\lambda = 0.71 \pm 0.01. \quad (8)$$

This value is significantly larger than the theoretical prediction (7). In this comparison, however, it should be kept in mind that (6) is only valid asymptotically for large  $N$ . We have checked for a systematic trend in our data by discarding more and more points for small  $N$  in the fits. As a result we observe only a slight trend to smaller values of  $1/\lambda$ , which is hardly significant in view of the increasing error bars. Single fits to all data points gave compatible results. In a recent MC study of the cosine formulation Schmidt and Schneider<sup>8</sup> obtained from an analysis of Binder's parameter a similar value of  $1/\lambda = 0.70 \pm 0.08$ , albeit with a much larger error bar. In order to clarify the discrepancy with the theoretical prediction (7) it would be desirable to perform further simulations of much larger systems.

In Table I we also give the locations  $\beta_{\max}(N)$  of the specific-heat peaks. It is well known that in two dimensions the peak maximum stays finite in the infinite volume limit and that the peak location does not coincide with the transition point but is displayed by about 30% to higher temperatures. We see that with increasing film thickness  $N$  the absolute distance from  $\beta_c(N)$  decreases. Assuming that also  $\beta_{\max}(N)$  scales according to (6), three-parameter fits give an even larger exponent of  $1/\lambda \approx 0.8$  and favor a value of  $\beta_{\max}^{3D} \equiv \beta_{\max}(\infty) \approx 0.331$  that is slightly smaller than  $\beta_c^{3D} \approx 0.334$ . The quality of the fits, however, is much worse than in the case of  $\beta_c(N)$  and, by discarding data points for small  $N$ , this time a trend to lower values of  $1/\lambda$  and higher values of  $\beta_{\max}^{3D}$  is visible. In Fig. 3 we have adopted the quite plausible and commonly accepted hypothesis that  $\beta_{\max}^{3D} = \beta_c^{3D}$ . [Recalling that also in 3D the specific-heat peak is finite with a cusplike singularity (the critical exponent  $\alpha_{3D} = 2 - D\nu_{3D} \approx -0.01$  is slightly *negative*), we are, howev-

TABLE II. Three-parameter fits  $\beta_c(N) = \beta_c^{3D} + cN^{-\lambda}$ .

Fit	$\chi^2$	$Q$	$c$	$\beta_c^{3D}$	$1/\lambda$
$\xi(T)$	7.21	0.07	0.401(13)	0.3343(9)	0.706(19)
$\xi(\beta)$	8.24	0.04	0.407(15)	0.3344(10)	0.703(20)
$\chi(T)$	3.86	0.28	0.389(6)	0.3336(4)	0.725(8)
$\chi(\beta)$	2.02	0.57	0.397(6)	0.3334(4)	0.721(9)

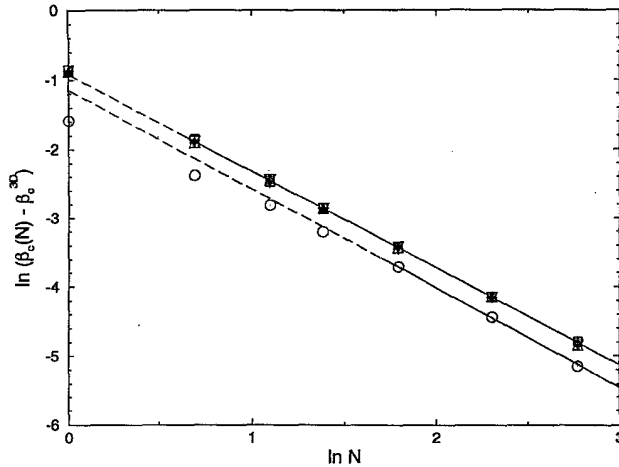


FIG. 3. Scaling of  $\beta_c(N)$  with  $N$ , calculated from KT fits to  $\xi(T)$  (+),  $\xi(\beta)$  ( $\square$ ),  $\chi(T)$  ( $\triangle$ ), and  $\chi(\beta)$  ( $\nabla$ ). Also shown are the peak locations  $\beta_{\max}(N)$  of the specific heat ( $\circ$ ).

er, not aware of a precise mathematical argument enforcing this equality]. While for small  $N$  a curvature is obvious in the data ( $\circ$ ) for  $\beta_{\max}(N)$ , the linear fit through the last three points looks reasonable and gives an exponent compatible with (8),  $1/\lambda=0.70(1)$ .

Let us finally discuss the topological defect structure in the film geometry. Since geometrically the films are 3D, the topological excitations are vortex lines. On the other hand one expects that near criticality these lines should behave effectively like the vortex points invoked in the KT picture. One possible scenario advanced in the literature<sup>26</sup> is that these lines degenerate near criticality to rod-like objects in the  $z$  direction, such that the projection onto the  $xy$  plane should look like a gas of vortex points (with the correct logarithmic long-range interaction derived from a summation over the  $1/r$  interactions between all line elements, similar to the treatment of parallel currents in electrodynamics). The vortex line distributions displayed in Fig. 4 clearly show that this explanation does not work. In fact, corresponding plots for the pure 3D case<sup>14</sup> look quite similar. For a finite number of layers, the interaction potential between vortex lines is easily seen to be anisotropic with explicit logarithmic terms. To understand the entropic contributions, however, is a difficult problem which requires further considerations.

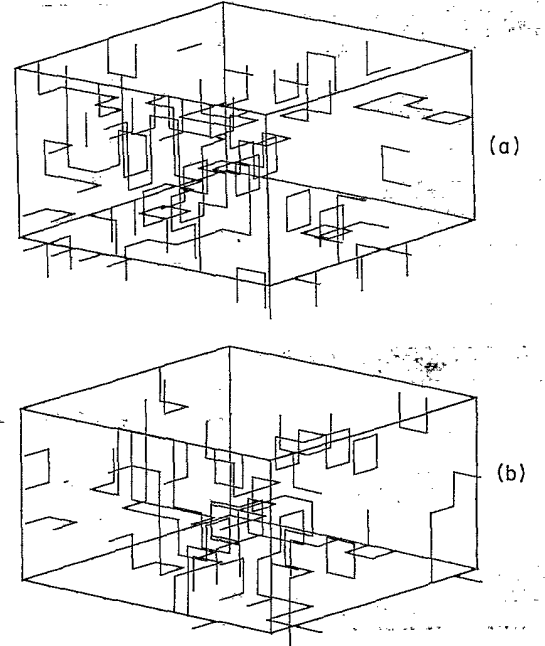


FIG. 4. Vortex lines in a  $6 \times 10^2$  section of a  $6 \times 200^2$  lattice at (a)  $\beta=0.355$  ( $\xi \approx 19$ ) and (b)  $\beta=0.366 \approx \beta_c$ .

## V. CONCLUDING REMARKS

To summarize, for films of  $XY$  spins in the periodic Gaussian formulation with up to  $N=16$  layers and free boundary conditions in the  $z$  direction, we observe a pronounced scaling of the critical couplings with  $N$ . The associated critical exponent, however, is not in agreement with theoretical expectations. A possible explanation of this discrepancy is that our films are not yet thick enough to see the true asymptotic scaling behavior.

Experimental studies of liquid-helium films, however, could also not confirm the theoretical prediction. Rather, while in early work<sup>27</sup> a value of  $1/\lambda=0.71 \pm 0.05$  is quoted, more recent studies<sup>28</sup> gave a much smaller value of  $1/\lambda=0.52 \pm 0.01$ .<sup>29</sup>

## ACKNOWLEDGMENTS

W.J. would like to thank Professor V. Dohm for a useful discussion and the Deutsche Forschungsgemeinschaft for financial support. This work was supported in part by Deutsche Forschungsgemeinschaft under Grant No. K1256.

<sup>1</sup>R. B. Griffiths, Phys. Rev. Lett. **24**, 1479 (1970).

<sup>2</sup>M. E. Fisher, in *Critical Phenomena*, Proceedings of the International School of Physics "Enrico Fermi," Varenna, Italy, Course LI, edited by M. S. Green (Academic, New York, 1971); T. W. Capehart and M. E. Fisher, Phys. Rev. B **13**, 5021 (1976).

<sup>3</sup>V. Ambegaokar, B. I. Halperin, D. R. Nelson, and E. D. Siggia, Phys. Rev. B **21**, 1806 (1980).

<sup>4</sup>K. Binder and P. C. Hohenberg, Phys. Rev. B **6**, 3461 (1972); **9**, 2194 (1974); K. Binder, Thin Solid Films **20**, 367 (1973).

<sup>5</sup>V. G. Vaks and A. I. Larkin, Zh. Eksp. Teor. Fiz. **49**, 975 (1965) [Sov. Phys. JETP **22**, 678 (1966)]; R. G. Bowers and G. S. Joyce, Phys. Rev. Lett. **19**, 630 (1967).

<sup>6</sup>J. Villain, J. Phys. (France) **36**, 581 (1975).

<sup>7</sup>W. Janke and K. Nather, in *Computer Simulation Studies in Condensed Matter Physics V*, Proceedings of the Workshop, 1992, Athens, Georgia, edited by D. P. Landau, K. K. Mon, and H.-B. Schüttler, Springer Proceedings in Physics **75** (Springer-Verlag, Berlin, 1993), p. 140.

<sup>8</sup>A. Schmidt and T. Schneider, Z. Phys. B **87**, 265 (1992); J.

- Phys. Soc. Jpn. **61**, 2169 (1992).
- <sup>9</sup>R. Savit, *Rev. Mod. Phys.* **52**, 453 (1980).
- <sup>10</sup>H. Kleinert, *Gauge Fields in Condensed Matter* (World Scientific, Singapore, 1989), Vol. I.
- <sup>11</sup>S. Ami and H. Kleinert, *Phys. Rev. B* **33**, 4692 (1986).
- <sup>12</sup>J. M. Kosterlitz and D. J. Thouless, *J. Phys. C* **6**, 1181 (1973); V. L. Berezinskii, *Zh. Eksp. Teor. Fiz.* **61**, 1144 (1971) [*Sov. Phys. JETP* **34**, 610 (1972)].
- <sup>13</sup>J. M. Kosterlitz, *J. Phys. C* **7**, 1046 (1974).
- <sup>14</sup>W. Janke, *Int. J. Theor. Phys.* **29**, 1251 (1990).
- <sup>15</sup>M. Ferer, M. A. Moore, and M. Wortis, *Phys. Rev. B* **8**, 5205 (1973); J. Adler, C. Holm, and W. Janke, *Physica A* (to be published).
- <sup>16</sup>J. C. LeGuillou and J. Zinn-Justin, *Phys. Rev. B* **21**, 3976 (1980); *J. Phys. Lett. (Paris)* **46**, L137 (1985).
- <sup>17</sup>M. Hasenbusch and S. Meyer, *Phys. Lett. B* **241**, 238 (1990).
- <sup>18</sup>W. Janke, *Phys. Lett. A* **148**, 306 (1990).
- <sup>19</sup>A. Patrascioiu and E. Seiler, *Phys. Rev. Lett.* **60**, 875 (1988); E. Seiler, I. O. Stamatescu, A. Patrascioiu, and V. Linke, *Nucl. Phys. B* **305**, 623 (1988).
- <sup>20</sup>P. Butera, M. Comi, and G. Marchesini, *Phys. Rev. B* **33**, 4725 (1986); **40**, 534 (1989); M. Ferer and Z. Mo, *ibid.* **42**, 10 769 (1990); P. Butera and M. Comi, *ibid.* **47**, 11 969 (1993).
- <sup>21</sup>R. Gupta, J. DeLapp, G. G. Battrouni, G. C. Fox, C. F. Baillie, and J. Apostolakis, *Phys. Rev. Lett.* **61**, 1996 (1988); U. Wolff, *Nucl. Phys. B* **322**, 759 (1989); R. G. Edwards, J. Goodman, and A. D. Sokal, *ibid.* **354**, 289 (1991); A. Hulsebos, J. Smit, and J. C. Vink, *ibid.* **356**, 775 (1991); R. Gupta and C. Baillie, *Phys. Rev. B* **45**, 2883 (1992).
- <sup>22</sup>W. Janke and K. Nather, *Phys. Lett. A* **157**, 11 (1991); *Phys. Rev. B* **48**, 7419 (1993).
- <sup>23</sup>K. Nather, Diplom thesis, FU Berlin, 1991.
- <sup>24</sup>U. Wolff, *Phys. Rev. Lett.* **62**, 361 (1989).
- <sup>25</sup>U. Wolff, *Nucl. Phys. B* **334**, 581 (1990).
- <sup>26</sup>V. N. Popov, *Zh. Eksp. Teor. Fiz.* **64**, 672 (1973) [*Sov. Phys. JETP* **37**, 341 (1973)].
- <sup>27</sup>J. Maps and R. B. Hallock, *Phys. Rev. Lett.* **47**, 1533 (1981).
- <sup>28</sup>Y. Y. Yu, D. Finotello, and F. M. Gasparini, *Phys. Rev. B* **39**, 6519 (1988).
- <sup>29</sup>For a recent review, see F. M. Gasparini and I. Rhee, in *Progress in Low Temperature Physics*, edited by D. F. Brewer (North-Holland, Amsterdam, 1992), Vol. XIII, p. 1.